

## Design, Synthesis, and Biological Evaluation of New Cyclic Disulfide Decapeptides That Inhibit the Binding of AP-1 to DNA

Keiichi Tsuchida,\*<sup>†</sup> Hisaaki Chaki,<sup>‡</sup> Tadakazu Takakura,<sup>†</sup> Junichi Yokotani,<sup>†</sup> Yukihiko Aikawa,<sup>‡</sup> Shunichi Shiozawa,<sup>§||</sup> Hiroaki Gouda,<sup>⊥</sup> and Shuichi Hirono<sup>⊥</sup>

Discovery Laboratories and Research Laboratories, Toyama Chemical Co., Ltd., 4-1 Shimookui 2-chome, Toyama 930-8508, Japan, Department of Rheumatology, Faculty of Health Science, Kobe University School of Medicine, 7-10-2 Tomogaoka, Suma-ku, Kobe 654-0142, Japan, Rheumatic Disease Division, Kobe University Hospital, 7-5-2 Kusunoki-cho, Chuo-ku, Kobe 650-0017, Japan, and School of Pharmaceutical Sciences, Kitasato University, 5-9-1 Shirokane, Minato-ku, Tokyo 108-8641, Japan

Received February 4, 2004

The transcription factor activator protein-1 (AP-1) is an attractive target for the treatment of immunoinflammatory diseases, such as rheumatoid arthritis. Using the three-dimensional (3D) X-ray crystallographic structure of the DNA-bound basic region leucine zipper (bZIP) domains of AP-1, new cyclic disulfide decapeptides were designed and synthesized that demonstrated AP-1 inhibitory activities. The most potent inhibition was exhibited by Ac-c[Cys-Gly-Gln-Leu-Asp-Leu-Ala-Asp-Gly-Cys]-NH<sub>2</sub> (peptide **2**) (IC<sub>50</sub> = 8 μM), which was largely due to the side chains of residues 3–6 and 8 of the peptide, as shown by an alanine scan. To provide structural information about the biologically active conformation of peptide **2**, the structures of peptide **2** derived from molecular dynamics simulation of the bZIP–peptide **2** complex with explicit water molecules were superimposed on the solution structures derived from NMR measurements of peptide **2** in water. These showed a strong structural similarity in the backbones of residues 3–7 and enabled the construction of a 3D pharmacophore model of AP-1 binding compounds, based on the chemical and structural features of the amino acid side chains of residues 3–7 in peptide **2**.

### Introduction

Activator protein-1 (AP-1) is an important transcription factor for genes involved in immune and inflammatory responses, such as cytokines and collagenase.<sup>1–3</sup> Various inflammatory and mitogenic stimulations lead to AP-1 activation, and it probably plays a role in rheumatoid arthritis, transplant rejection, and tumor growth, so it is an attractive therapeutic target for the treatment of such disorders.<sup>4</sup> Indeed, systematic administration of an AP-1 decoy oligodeoxynucleotide containing the AP-1 binding site was found to inhibit arthritic joint destruction in mice with collagen-induced arthritis.<sup>5</sup> AP-1 is composed of members of the Fos and Jun families.<sup>1</sup> Fos and Jun proteins dimerize through a leucine zipper motif at their carboxyl terminals and bind DNA through a basic region that is located immediately upstream of the leucine zipper.<sup>1,6</sup> The three-dimensional (3D) X-ray crystallographic structure<sup>7</sup> of the basic region leucine zipper (bZIP) domains of c-Fos and c-Jun bound to a 20 nucleotide DNA duplex containing the AP-1 binding site revealed single α-helices and showed that the heterodimer grips the major groove of the DNA like a pair of forceps. Although the solution structure of the bZIP domains of AP-1 in the absence of DNA is unclear, the effect of dimerization and DNA

binding on circular dichroism (CD) spectra of the bZIP domains suggested that the basic regions of the domains take on an α-helical conformation only in the presence of DNA.<sup>8</sup> In support of this, the solution structure of the yeast transcriptional factor GCN4 bZIP domain, as determined by NMR, revealed that the leucine zipper region forms a long uninterrupted α-helix and the basic region is flexible but structured, fluctuating around a helical conformation in the absence of DNA.<sup>9</sup>

Structure-based drug design methods have strongly enhanced the lead discovery and optimization process using the 3D structures of target proteins, which are important for understanding the interaction between the ligand and the target protein.<sup>10,11</sup> Recently, natural products such as curcumin,<sup>12,13</sup> dihydroguaiaretic acid,<sup>12,14</sup> momordin,<sup>15</sup> and a new anthraquinone derivative<sup>16</sup> were reported to inhibit the binding of AP-1 to the AP-1 binding site. However, 3D structural information about the AP-1 binding of these inhibitors is not yet available.

We therefore carried out the de novo design of cyclic peptides exhibiting AP-1 inhibitory activity using the 3D structure of the bZIP domains from the X-ray crystal structure of the AP-1–DNA complex.<sup>7</sup> Our aim was to construct a hypothetical 3D pharmacophore model for generating new AP-1 inhibitors. A pharmacophore model is defined as the 3D arrangement of the structural and physicochemical features that are relevant to biological activity and is a versatile tool to aid in the discovery and development of new lead compounds.<sup>17</sup>

Cyclization of a flexible linear peptide is known to reduce the conformational freedom of the peptide and restrict its possible conformations, often resulting in

\* To whom correspondence should be addressed. Tel: +81-76-431-8218. Fax: +81-76-431-8208. E-mail: KEIICHI\_TUCHIDA@toyama-chemical.co.jp.

<sup>†</sup> Discovery Laboratories, Toyama Chemical Co., Ltd.

<sup>‡</sup> Research Laboratories, Toyama Chemical Co., Ltd.

<sup>§</sup> Kobe University School of Medicine.

<sup>||</sup> Kobe University Hospital.

<sup>⊥</sup> Kitasato University.

higher receptor binding affinity.<sup>18,19</sup> Several methods for cyclization are known, and we selected the disulfide method, which forms a side chain–side chain disulfide bridge between the N- and the C-terminal Cys residues.

Here, we report the rational design and synthesis of cyclic disulfide decapeptides and their inhibitory activities as evaluated by an AP-1 binding assay. Ac-c[Cys-Gly-Gln-Leu-Asp-Leu-Ala-Asp-Gly-Cys]-NH<sub>2</sub> (peptide **2**) exhibited the most potent inhibitory activity (IC<sub>50</sub> = 8 μM) among these peptides. Furthermore, we built a pharmacophore model based on the chemical and structural features of peptide **2** obtained from an alanine scan and structural studies using a combination of NMR and molecular dynamics (MD) simulations of peptide **2**.

## Methods

**Molecular Modeling and de Novo Design.** The crystallographic coordinates of the bZIP domains of AP-1 were obtained from the Brookhaven Protein Data Bank, entry 1FOS,<sup>7</sup> followed by the addition of hydrogen atoms to the bZIP domains with standard geometry. All molecular modeling and docking studies were performed using the SYBYL software package version 6.4<sup>20</sup> running on a Silicon Graphics Power Indigo2 workstation. All of the peptides used in this study were built using the Biopolymer module. The designed peptides were N-terminal-acetylated and C-terminal-amidated. Ionizable residues in the bZIP domains and designed peptides were assumed to be charged under physiological conditions. Docking was performed with the manual docking module DOCK. Our design was based on the AP-1 DNA binding site topology from the X-ray crystal structure of the AP-1–DNA complex. In the complex, Asn147 and Arg155 of c-Fos and Asn271 of c-Jun interact with the bases of the AP-1 binding site by hydrogen bonds, whereas the β-carbons of Ala150, Ala151 and Ser154 of c-Fos and Ala274, Ala275 and Ser278 of c-Jun come in contact with the 5-methyl groups of thymine bases of the AP-1 binding site by hydrophobic interactions.<sup>7</sup> The residues involved in these interactions are essential for the high-affinity binding of AP-1 to DNA.<sup>21–26</sup> On the basis of these interactions between the bZIP domains and the DNA, the candidate peptides were manually docked in the binding site. In particular, several spatial orientations and conformations of peptides were evaluated in the binding site of the bZIP domains.

Minimization of each complex obtained by docking was performed to reach a final convergence of 0.001 kcal mol<sup>-1</sup> Å<sup>-1</sup> by the Powell method in the MAXIMIN2 module of SYBYL. The Tripos force field<sup>27</sup> was used for the energy minimizations, and a dielectric constant of 78.3 was employed. Partial atomic charges were calculated by the method of Gasteiger and Hückel.<sup>28,29</sup> The intermolecular energy of the peptide–binding site interaction was used to evaluate the quality of the docking experiment.

**MD Simulations.** The MD calculations were performed with AMBER version 4.1.<sup>30</sup> The structure of the bZIP–peptide **1** (Ac-c[Cys-Gly-Gln-Leu-Asp-Leu-Ala-Leu-Gly-Cys]-NH<sub>2</sub>) complex obtained by docking was covered with an 18 Å shell of 9163 water molecules. The TIP3P model was used as the water model.<sup>31</sup> The

resulting structure of the complex was optimized using energy minimization until the root-mean-square (RMS) value of the potential gradient was <0.05 kcal mol<sup>-1</sup> Å<sup>-1</sup>. MD simulation was then performed for 100 ps at 310 K with a dielectric constant of 1.0. Next, the initial structure of the bZIP–peptide **2** complex was constructed by the replacement of Leu in position 8 of peptide **1** with Asp while maintaining the original side chain orientation in the bZIP–peptide **1** complex after removing water molecules using the Biopolymer module of SYBYL 6.4. The structure obtained was covered with a 22 Å shell of 12 810 water molecules. After energy minimization of the structure, MD simulation was carried out for a period of 400 ps. The model structure obtained after MD simulation was minimized using the conditions described above.

The SHAKE algorithm was employed to restrain the bond lengths in order to remove the high-frequency motions.<sup>32</sup> This allowed us to use a time step of 1 fs. We used the dual nonbonded cutoff method with a primary cutoff of 9 Å and a secondary cutoff of 12 Å. The nonbonded pair list was updated every 20 time steps in the MD calculations. All calculations were carried out using a Silicon Graphics Power Indigo2 workstation.

## Results and Discussion

**De Novo Design.** We designed candidate peptides using a combination of aliphatic hydrophobic amino acids such as Leu, Ile, and Val, acidic amino acids such as Asp and Glu, and neutral polar amino acids such as Asn and Gln. bZIP domains lack a binding cavity, so we chose a manual rather than an automated docking procedure. First, we searched for a tripeptide to interact with the residues, Asn147, Ala150, Ala151, Ser154, and Arg155 in the basic region of c-Fos, which participate in contacts with the bases of the AP-1 binding site of DNA. We chose Ac-Asn-Leu-Asp-NH<sub>2</sub> to assume the hydrogen-bonding interaction between the Asn residue and the Asn147 and between the Asp residue and the Arg155 and the hydrophobic interaction between the Leu residue and the residues, Ala150, Ala151, and Ser154, and then, we docked the tripeptide into the binding site of the bZIP domains (Figure 1a). Next, we elongated the tripeptide stepwise at the C terminus by one residue increments to the hexapeptide Ac-Asn-Leu-Asp-Leu-Ala-Leu-NH<sub>2</sub> to interact with the residues Asn271, Ala274, Ala275, and Ser278 in the basic region of c-Jun. Finally, we built the cyclic disulfide decapeptide Ac-c[Cys-Gly-Asn-Leu-Asp-Leu-Ala-Leu-Gly-Cys]-NH<sub>2</sub> by addition of Cys-Gly residues at the N terminus and Gly-Cys residues at the C terminus to the hexapeptide and by cyclization of the resulting decapeptide. On the basis of the docking model of the cyclic peptide, we designed several cyclic peptides by replacement of a residue of the cyclic peptide by appropriate residue to assume an interaction with the putative binding site in the bZIP domains. By way of example, Figure 1b shows the docking model of peptide **1**, obtained by replacement of Asn3 with Gln and energy minimization. After evaluating the quality of the docking experiment by the interaction energy between the designed peptide and the bZIP domains, decapeptides with relatively large interaction energies were synthe-

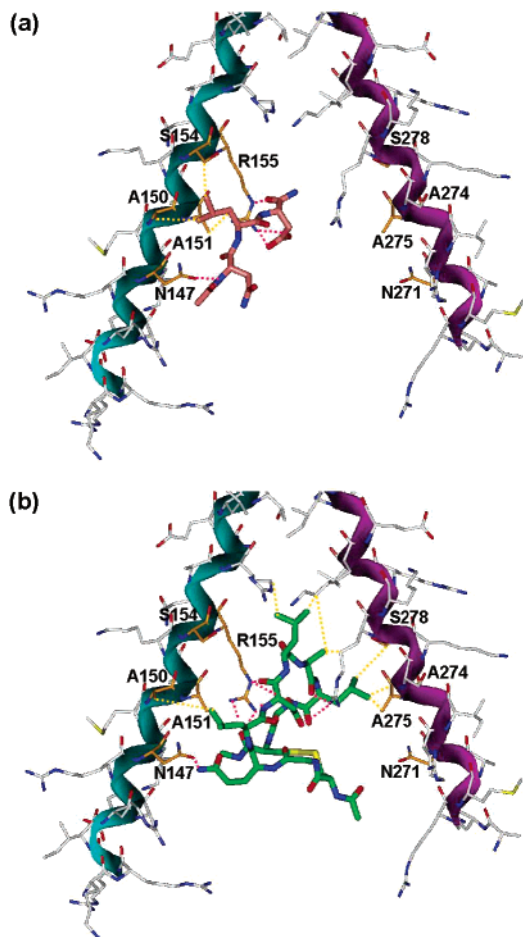


**Figure 1.** Docking models of the designed peptides with the binding site in the bZIP domains. (a) Ac-Asn-Leu-Asp-NH<sub>2</sub>, pink; (b) peptide **1**, green. Ribbon representation of the Fos and Jun basic regions (c-Fos, cyan; c-Jun, magenta). Orange residues, residues involved in AP-1–DNA interactions; red broken lines, putative hydrogen bonds; yellow broken lines, putative hydrophobic interactions.

sized using the standard solid phase methodology with Fmoc chemistry and were evaluated using AP-1 binding assays in which peptides competed for the binding of digoxigenin (DIG)-labeled oligonucleotides containing the AP-1 binding site. Among these peptides, peptide **1** exhibited a weak inhibitory activity at 1 mM, whereas the corresponding linear peptide Ac-Gln-Leu-Asp-Leu-Ala-Leu-NH<sub>2</sub> exhibited no inhibitory activity at same concentration. It was assumed that cyclization of the flexible linear peptide converted it from an inactive to an active conformation.

Next, we performed the MD simulation of the bZIP–peptide **1** complex obtained by docking in order to relax the structure. The resulting structure of the complex from the MD simulation at 100 ps is shown in Figure 2. On the basis of the complex structure after 100 ps, we designed several cyclic peptides to interact more strongly with the putative binding site in the bZIP domains. Replacement of Leu with Asp in position 8 of peptide **1** resulted in Ac-c[Cys-Gly-Gln-Leu-Asp-Leu-Ala-Asp-Gly-Cys]-NH<sub>2</sub> (peptide **2**), which was found to possess a more potent inhibitory activity (IC<sub>50</sub> = 8 μM).

We synthesized analogues of peptide **2** in which each Gly was deleted to reduce the ring size and produce more constrained cyclic decapeptides. However, each

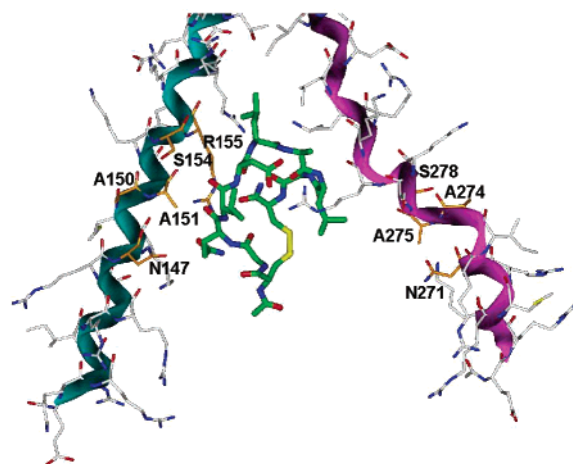


**Figure 2.** Snapshot taken from MD simulation of the bZIP–peptide **1** complex at 100 ps. The color coding is the same as in Figure 1.

resulting cyclic nonapeptide (Table 1; peptides **3** and **4**) demonstrated a significant loss of inhibitory activity. It was assumed that reduction of the ring size of the peptide backbone altered the peptide from an active to an inactive conformation.

**Alanine Scan of Peptide 2.** To evaluate the contributions of each of the amino acid side chains, we synthesized analogues of peptide **2** in which each residue, except for Cys, was substituted with Ala (Table 1; peptides **5**–**11**). This strategy has recently been used to identify the amino acid side chains participating in ligand–receptor interactions while preserving the configuration of the peptide backbone and maintaining a similar conformation.<sup>33–36</sup> Substitutions of Leu4, Asp5, Leu6, and Asp8 by Ala resulted in a nearly complete loss of inhibitory activities at 100 or 200 μM. Substitution of Gln3 by Ala resulted in only weak inhibitory activity. Substitution of the aspartic acid side chain in position 5 showed the greatest effect. These results indicate that side chains of Gln3, Leu4, Asp5, Leu6, and Asp8 in peptide **2** contribute significantly to inhibitory activity against the binding of AP-1 to DNA. Peptides **5** and **11**, in which each Gly residue had been substituted by Ala, were devoid of inhibitory activities. It was assumed that replacement of Gly by Ala, which is expected to restrict the conformational freedom of the peptide backbone at this point, changed the active conformation of the peptide to an inactive form.

**Modification of Peptide 2.** Although an alanine scan is useful for identifying important side chains, such analogues provide little information about the nature of the interactions or indirect effects due to changes in the peptide structure. To examine optimal side chains and obtain a more potent inhibitor, we synthesized analogues in which each side chain in peptide **2** was substituted with a more subtle isosteric or isoelectronic amino acid (Table 1; peptides **12**–**18**).

Gln3 was substituted with Glu or Lys (peptides **12** and **13**), resulting in complete loss of inhibitory activity at 200 μM. Substitution with Asn, causing contraction of the carboxamide side chain (peptide **14**), resulted in a moderate loss of inhibitory activity (>10-fold).

Substitution of Leu with the more hydrophobic amino acid cyclohexylalanine (Cha) (peptides **15** and **16**) resulted in a nearly complete loss of inhibitory activity.

**Table 1.** Analytical Data and Percentages of Inhibition at 100  $\mu$ M and IC<sub>50</sub> of Synthetic Peptides (**2**–**18**) of the Form Ac-c[Cys-A<sup>2</sup>-A<sup>3</sup>-A<sup>4</sup>-A<sup>5</sup>-A<sup>6</sup>-A<sup>7</sup>-A<sup>8</sup>-A<sup>9</sup>-Cys]-NH<sub>2</sub>

peptide	sequence								MS		HPLC $t_R$ (min) <sup>d</sup>		% inhibition at 100 $\mu$ M	IC <sub>50</sub> ( $\mu$ M)
	A <sup>2</sup>	A <sup>3</sup>	A <sup>4</sup>	A <sup>5</sup>	A <sup>6</sup>	A <sup>7</sup>	A <sup>8</sup>	A <sup>9</sup>	calcd <sup>a</sup>	obsd <sup>b</sup>	method 1	method 2		
<b>2</b>	Gly	Gln	Leu	Asp	Leu	Ala	Asp	Gly	1033.4	1033.8	11.42	8.76	81	8
<b>3</b>		Gln	Leu	Asp	Leu	Ala	Asp	Gly	974.4 <sup>c</sup>	974.8 <sup>c</sup>	11.06	9.47	-2	>100
<b>4</b>	Gly	Gln	Leu	Asp	Leu	Ala	Asp	Gly	974.4 <sup>c</sup>	974.8 <sup>c</sup>	11.12	9.72	11	>100
<b>5</b>	Ala	Gln	Leu	Asp	Leu	Ala	Asp	Gly	1047.4	1047.3	11.34	9.51	5	>100
<b>6</b>	Gly	Ala	Leu	Asp	Leu	Ala	Asp	Gly	976.4	976.8	12.36	11.10	29	>100
<b>7</b>	Gly	Gln	Ala	Asp	Leu	Ala	Asp	Gly	991.4	991.3	8.00	3.44	11	>100
<b>8</b>	Gly	Gln	Leu	Ala	Leu	Ala	Asp	Gly	989.4	989.9	10.86	8.86	-1 <sup>e</sup>	>200
<b>9</b>	Gly	Gln	Leu	Asp	Ala	Ala	Asp	Gly	991.4	991.9	7.33	3.44	7	>100
<b>10</b>	Gly	Gln	Leu	Asp	Leu	Ala	Ala	Gly	989.4	989.9	11.38	9.85	14	>100
<b>11</b>	Gly	Gln	Leu	Asp	Leu	Ala	Asp	Ala	1047.4	1047.5	11.65	10.12	15	>100
<b>12</b>	Gly	Glu	Leu	Asp	Leu	Ala	Asp	Gly	1034.4	1034.4	11.44	10.14	-2 <sup>e</sup>	>200
<b>13</b>	Gly	Lys	Leu	Asp	Leu	Ala	Asp	Gly	1033.4	1033.6	10.13	7.78	-2 <sup>e</sup>	>200
<b>14</b>	Gly	Asn	Leu	Asp	Leu	Ala	Asp	Gly	1019.4	1019.8	10.55	8.34	42	>100
<b>15</b>	Gly	Gln	Cha	Asp	Leu	Ala	Asp	Gly	1073.4	1073.4	13.40	14.44	-22	>100
<b>16</b>	Gly	Gln	Leu	Asp	Cha	Ala	Asp	Gly	1073.4	1073.4	13.61	14.68	10	>100
<b>17</b>	Gly	Gln	Leu	Asp	Leu	Gly	Asp	Gly	1019.4	1019.4	10.32	8.31	1 <sup>e</sup>	>200
<b>18</b>	Gly	Gln	Leu	Asp	Leu	Ala	Asn	Gly	1032.4	1032.8	10.93	7.72	64	52

<sup>a</sup> Theoretical molecular mass (M + H<sup>+</sup>, Da) except for **3** and **4**. <sup>b</sup> Observed molecular mass (M + H<sup>+</sup>, Da) except for **3** and **4**. <sup>c</sup> (M - H<sup>+</sup>, Da). <sup>d</sup> Retention time (see Experimental Section). <sup>e</sup> Synthetic peptides were assayed at 100  $\mu$ M except for **8**, **12**, **13**, and **17** (at 200  $\mu$ M).

At these positions, Leu would be suitable for the interaction with AP-1. Substitution of Ala7 with Gly (peptide **17**) resulted in a complete loss of inhibitory activity. The methyl side chain of Ala might participate in the interaction with AP-1, or the replacement with Gly might change the active conformation of the peptide to an inactive form.

Asp8 was substituted with Asn (peptide **18**), resulting in a moderate loss of inhibitory activity (6.5-fold). At this position, the charge-charge interaction with AP-1 would be more favorable. Of the peptides tested in this study, peptide **2** emerged as that with the most potent inhibitory activity against the binding of AP-1 to DNA.

### Three-Dimensional Pharmacophore Modeling.

To obtain 3D structural information for the active conformation of peptide **2**, we carried out a MD simulation of the bZIP-peptide **2** complex with explicit water molecules and NMR measurements of peptide **2** in water. The MD simulation was run for 400 ps until the system was equilibrated. Six snapshots, extracted at 10 ps intervals from the last 50 ps MD simulation, were similar to one another in terms of RMS deviation for all backbone N, C <sub>$\alpha$</sub> , C, and O atoms (mean  $\pm$  SD = 1.85  $\pm$  0.48 Å). Peptide **2** was stable during the last 50 ps of the MD simulation, and the average RMS deviations between each of the six snapshots for all backbone atoms and all heavy atoms were 0.65  $\pm$  0.17 and 0.89  $\pm$  0.13 Å, respectively.

The binding model of peptide **2** at 400 ps is presented in Figure 3. The leucine zipper region retained approximately 70% of the  $\alpha$ -helical conformation at the carboxyl terminal, whereas the basic regions underwent a partial change to a random coil conformation, in particular for the c-Jun domain. This is similar to information obtained by CD and NMR about the solution structure of the AP-1 or GCN4 bZIP domains in the absence of DNA.<sup>8,9</sup> We speculate that the binding mode of peptide **2** with the bZIP domains is different from that of its binding to DNA.

The sequence-specific NMR assignment of peptide **2** was achieved according to the standard method established by Wüthrich.<sup>37</sup> Identification of amino acid spin systems was based on DQF-COSY<sup>38</sup> and TOCSY<sup>39</sup>

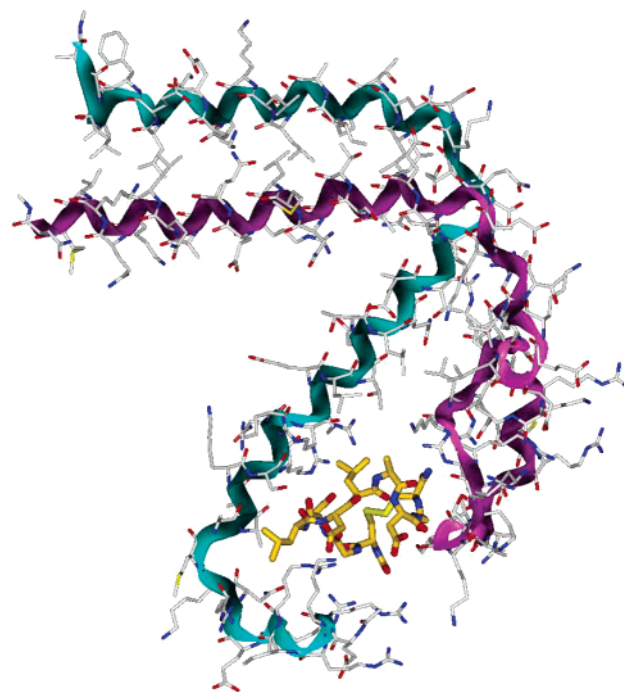


**Figure 3.** Binding model of peptide **2** (yellow) resulting from MD simulation at 400 ps. Ribbon representation of the bZIP domains (c-Fos, cyan; c-Jun, magenta).

spectra and complemented with the results of NOESY<sup>40</sup> experiments. Starting with the unique residue Ala7, which could be easily identified on the basis of its spin type, sequential connectivities were carried out by the analysis of the C <sub>$\alpha$</sub> H<sub>( $j$ )</sub>-NH<sub>( $i+1$ )</sub> (d <sub>$\alpha$ N</sub>) and NH<sub>( $j$ )</sub>-NH<sub>( $i+1$ )</sub> nuclear Overhauser effects (NOEs). Figure 4 shows the C <sub>$\alpha$</sub> H-NH fingerprint region of the NOESY spectrum containing sequential d <sub>$\alpha$ N</sub> connectivities. The proton chemical shifts of peptide **2** are summarized in Table 2.

For solution structure determination of peptide **2**, 12 intrareidual, 37 sequential, 19 medium range ( $|i - j| < 5$ , where  $i$  and  $j$  are residue numbers), and three long range ( $|i - j| \geq 5$ ) NOEs were detected and converted to the distance constraints. On the basis of the <sup>3</sup>J(H-C <sub>$\alpha$</sub> -C <sub>$\beta$</sub> -H) coupling constants and the intensities of

**Table 2.**  $^1\text{H}$  Chemical Shifts<sup>a</sup> (ppm) for Peptide **2** at 5 °C and pH 4.65

residue	NH	H <sub>α</sub>	H <sub>β</sub>	others
CH <sub>3</sub> <sup>b</sup>		2.02		
Cys1	8.62	4.64	3.00 (β <sub>2</sub> ), 3.19 (β <sub>3</sub> )	
Gly2	8.89	3.95		
Gln3	8.37	4.26	1.98 (β <sub>2</sub> ), 2.11 (β <sub>3</sub> )	C <sub>γ</sub> 2.33; C <sub>ε</sub> 6.92, 7.66
Leu4	8.33	4.28	1.57, 1.70	C <sub>γ</sub> 1.57; C <sub>δ</sub> 0.82, 0.88
Asp5	8.14	4.54	2.68, 2.84	
Leu6	8.17	4.29	1.58, 1.65	C <sub>γ</sub> 1.57; C <sub>δ</sub> 0.82, 0.88
Ala7	8.28	4.23	1.38	
Asp8	8.21	4.58	2.69 (β <sub>3</sub> ), 2.77 (β <sub>2</sub> )	
Gly9	8.34	3.87, 4.02		
Cys10	8.25	4.60	3.00 (β <sub>2</sub> ), 3.21 (β <sub>3</sub> )	
NH <sub>2</sub> <sup>b</sup>	7.27, 7.77			

<sup>a</sup> Chemical shifts are relative to the water resonance located at 4.95 ppm. <sup>b</sup> Peptide **2** has an acetylated N terminus and an amidated C terminus.

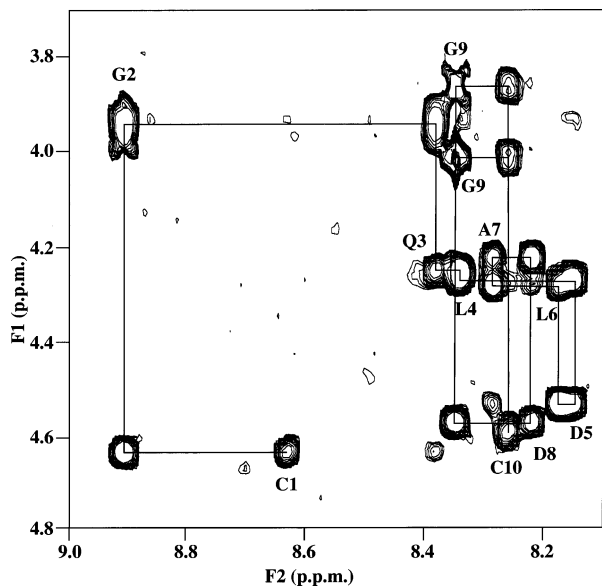


**Figure 4.** Sequential NOE connectivities for residues 1–10 of peptide **2** in the NOESY spectrum observed with a mixing time of 500 ms at 5 °C. Intraresidue NH-C<sub>α</sub>H cross-peaks are labeled with the residue number by standard single-letter amino acid abbreviations.

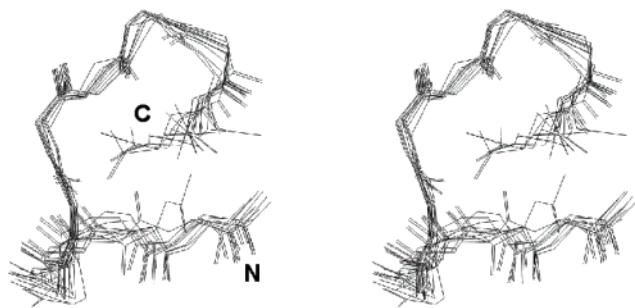


**Figure 5.** Stereoview of the superimposition of the 11 converged structures of the major cluster of peptide **2**. These are the results of the best fit of all backbone N, C<sub>α</sub>, C, and O atoms.

intramolecular NOEs, we established the stereospecific assignments of the prochiral β-methylene protons and the range of the  $\chi_1$  side chain dihedral angles for Cys1, Gln3, Asp8, and Cys10. A total of 75 NMR constraints, which consisted of 71 distance constraints and four dihedral angle constraints, were used for the following simulated annealing calculations.

A set of 200 individual structures was calculated on the basis of the NMR experimental constraints. These

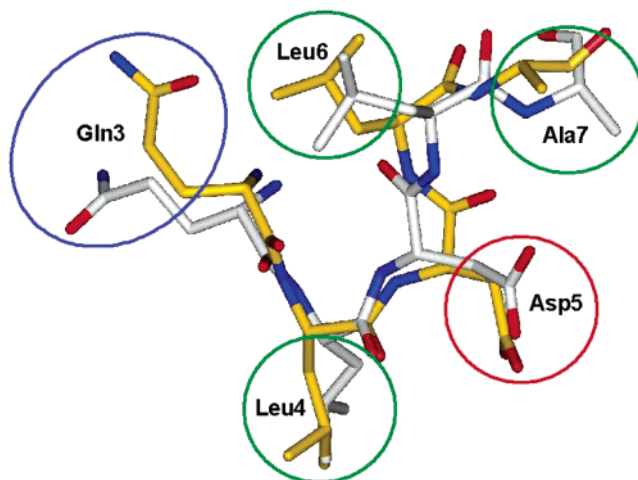


**Figure 6.** Superimposition of Gln3-Leu4-Asp5-Leu6-Ala7 of peptide **2** of the lowest energy conformer obtained by NMR (white) and MD simulation-derived structure at 400 ps (yellow). These are the results of the best fit of the backbone atoms. Three-dimensional pharmacophore model of AP-1 binding compounds: green, hydrophobic groups; blue, hydrogen donor or acceptor group; and red, acidic group.

calculations provided 17 structures that had no distance violations  $>0.2$  Å and no dihedral angle violations  $>5^\circ$ . The resulting conformations were grouped into three clusters according to the pairwise RMS deviations between 17 individual structures. Figure 5 shows a stereoview of the best-fit superimposition of the backbone atoms for the 11 individual converged structures of the major cluster. The average pairwise RMS deviation between the 11 structures was  $1.18 \pm 0.54$  Å for all backbone atoms.

Here, we hypothesized that the rigid part of the cyclic peptide solution structure might be conserved in the biologically active conformation. Superimposition studies showed that the MD simulation-derived structures of peptide **2** in the complex were similar to the major cluster of the NMR-determined solution structures of peptide **2** in the backbones of the sequence Gln3-Leu4-Asp5-Leu6-Ala7 ( $1.45 \pm 0.10$  Å). Among these residues, the side chains of Glu3, Leu4, Asp5, and Leu6 have been shown by the alanine scan experiment to be important for inhibitory activity, as described above. Although it is unknown whether Ala7 is involved in the hydrophobic interaction with AP-1, we assumed that it contributes to the observed inhibitory activity.

From these results, we built a 3D pharmacophore model of AP-1 binding compounds, based on the chemi-

cal and structural features of the amino acid side chains of residues 3–7 in peptide **2** (Figure 6). The pharmacophore consists of three hydrophobic groups, one hydrogen bond acceptor or donor, and one acidic group. This 3D model will be useful in the process of molecular design and the search of 3D databases to identify the chemical structures of potential novel AP-1 inhibitors.

## Conclusions

In the absence of precise 3D structural information about AP-1, a combination of the available experimental data and molecular modeling methods—such as docking and MD simulations—was used to design novel inhibitors of AP-1. The computer-aided molecular design strategies used in the present study produced novel cyclic decapeptides that exhibited AP-1 inhibitory activity. Such peptides will prove useful as intermediates in the search for nonpeptide and small molecule inhibitors.

This study proposes a 3D pharmacophore model of AP-1 binding compounds. We aim to use our model to discover small molecule inhibitors of AP-1 based on de novo design or 3D database searches. Although this model relies on many hypotheses and remains speculative, the current successful development of nonpeptide inhibitors lends credibility to the 3D pharmacophore model of AP-1 binding compounds.

## Experimental Section

**Abbreviations.** Abbreviations of common amino acids and representations of peptides are in accordance with the recommendations of the IUPAC-IUB Joint Commission on Biochemical Nomenclature.<sup>41</sup> Additional abbreviations are used as follows: DMF, *N,N*-dimethylformamide; DMSO, dimethyl sulfoxide; Fmoc, 9-fluorenylmethoxycarbonyl; HPLC, high-performance liquid chromatography; mequiv, milliequivalent; *t*Bu, *tert*-butyl; TFA, trifluoroacetic acid; Trt, triphenylmethyl.

**Materials and Methods.** Rink Amide MBHA resin (0.55 mequiv/g) was obtained from NovaBiochem (Läufelfingen, Switzerland). All of the protected amino acids (Fmoc and Fmoc plus Trt or *t*Bu) and the coupling reagents were purchased from NovaBiochem. All purchased amino acids were of the L-configuration. All reagents and solvents were reagent grade or better and were used without further purification.

HPLC was performed with a Hitachi L-7100 apparatus equipped with an L-7400 UV detector (peak detection at 230 nm) using an ODS-AP column (YMC-Pack, YMC Co., Kyoto, Japan) of 250 mm × 20 mm for preparative or 150 mm × 4.6 mm for analytical HPLC, respectively. Liquid chromatography–electrospray ionization mass spectrometry was performed with a Finnigan 700 triple-sector quadrupole mass spectrometer equipped with a Waters 626 LC system and a Finnigan MAT electrospray ionization system (4.5 kV).

**Peptide Synthesis.** All peptides were synthesized manually using standard solid phase peptide chemistry<sup>42</sup> with Fmoc-protected amino acids<sup>43</sup> on Rink Amide MBHA resin<sup>44</sup> at a 0.2 mmol scale. Couplings with Fmoc amino acids (3 equiv) were performed in the presence of 1-hydroxybenzotriazole and 1,3-diisopropylcarbodiimide (each 3 equiv) in DMF (5 mL) at room temperature for 2 h, and then, the Fmoc protecting group was removed by treatment with 20% piperidine in DMF (5 mL) at room temperature for 20 min. After deprotection of the last Fmoc group on Cys(Trt), the peptide resin was treated with acetic anhydride and *N,N*-diisopropylethylamine (each 10 equiv) in a 1:1 mixture of DMF and CH<sub>2</sub>Cl<sub>2</sub> (5 mL) at room temperature for 30 min before filtration and washing with DMF (×4) and CH<sub>2</sub>Cl<sub>2</sub> (×3) followed by drying in vacuo. The terminal-*N*-acetyl product was treated with a mixture of TFA–thioanisole–water (92.5:5.0:2.5) (20 mL) at room temperature for 4 h to induce cleavage of the peptide from the

resin and removal of the remaining O- and S-protecting groups. The exhausted resin was filtered, the filtrate was mixed with ether (50 mL), and the precipitate was isolated by centrifugation.

A solution of the dithiol product in 10% DMSO in TFA (10 mL) was stirred at room temperature for 20 h before concentration to approximately 2 mL and the addition of ether (50 mL).<sup>45</sup> The precipitate was collected by centrifugation and purified by preparative reverse phase HPLC eluted with a linear gradient of acetonitrile in water containing 0.1% TFA at a flow rate of 8.0 mL/min before lyophilization. The homogeneity of the resulting peptides was tested by analytical HPLC using two solvent systems: method 1, 30 min gradient of 10–70% acetonitrile in 0.1% aqueous TFA; method 2, 30 min gradient of 35–95% methanol in 0.1% aqueous TFA. The purity of the peptides was determined by HPLC to be >95%. A summary of the analytical results for each peptide described in this paper is provided in Table 1.

**Enzyme-Linked DNA–Protein Interaction Assay.** The inhibition constants of the synthetic peptides for DNA binding activity of AP-1 were determined by an enzyme-linked DNA–protein interaction assay using synthetic double-stranded oligonucleotides, which contain the AP-1 binding site (shown in bold) and nuclear protein. The synthetic oligonucleotides 5'-CTAGTGATGAGTCAGCCGGATC-3' and 5'-GATCCGGC-TGACTCATACTAG-3' (Bio-Synthesis, Lewisville, TX) were labeled with DIG-ddUTP as described in the DIG oligonucleotide 3'-end-labeling kit (Boehringer Mannheim, Mannheim, Germany). After they were annealed, they were used as DIG-labeled double-stranded oligonucleotides. Nuclear extract proteins were prepared from phorbol myristate acetate-stimulated HeLa cells according to the protocol described by Dignam et al.<sup>46</sup> and were used after dialysis against reaction buffer [20 mM *N*-(2-hydroxyethyl)piperazine-*N*'-2-ethanesulfonic acid-KOH (pH 7.9) containing 0.5 mM ethylenediaminetetraacetic acid, 50 mM KCl, 0.5 mM dithiothreitol, 0.5 mM phenylmethylsulfonyl fluoride, and 10% (v/v) glycerol].

Ninety-six well microplates (Corning Inc., Corning, NY) were coated with nuclear extract (1 μg/mL; 100 μL/well) at 4 °C overnight. After they were washed with phosphate-buffered saline containing 0.05% Tween-20, DIG-labeled double-stranded oligonucleotides (10 pM) in reaction buffer were mixed with each sample dissolved in DMSO (99:1–98:2), and 100 μL of each mixture was added to the wells. After they were incubated for 1 h at room temperature, the wells were washed with reaction buffer containing 0.05% Tween-20. Horseradish peroxidase-conjugated goat anti-DIG antibody (0.04 units/mL, Boehringer Mannheim) in binding buffer containing 0.1% bovine serum albumin was added (100 μL/well) and incubated for 1 h at room temperature. *o*-Phenylenediamine (1 mg/mL) in 100 mM Na<sub>2</sub>HPO<sub>4</sub>/200 mM citric acid buffer (pH 5.0) containing 0.1% H<sub>2</sub>O<sub>2</sub> was added (100 μL/well), and the color reaction was allowed to develop for 20 min at room temperature. After 50 μL of 1 M H<sub>2</sub>SO<sub>4</sub> was added to each well to stop the reaction, the optical density was measured with a microplate reader (Bio-Rad model 450, Bio-Rad Laboratories, Hercules, CA) at a wavelength of 492 nm. The IC<sub>50</sub> values were calculated by a logistic concentration–response curve using the SAS System version 8.2 (SAS Institute Inc., Cary, NA).

**NMR Measurements and Simulated Annealing Calculations.** Peptide **2** (4 mg) was dissolved in 0.5 mL of either 90% H<sub>2</sub>O/10% D<sub>2</sub>O or D<sub>2</sub>O containing 50 mM CD<sub>3</sub>COONa. The sample solution was adjusted to pH 4.65. All NMR spectra were recorded on a Varian INOVA600 spectrometer operating at 600 MHz for a proton frequency at two temperatures: 5 and 25 °C. For spectral assignment and extraction of structural information, DQF-COSY,<sup>38</sup> TOCSY,<sup>39</sup> NOESY,<sup>40</sup> ROESY,<sup>47</sup> and E.COSY<sup>48</sup> experiments were performed in the phase sensitive mode.<sup>49</sup> The DQF-COSY and E.COSY spectra were recorded with 512 increments of 8K data points and 32 transients. The TOCSY spectra were recorded with mixing times of 20 and 50 ms. The NOESY spectra were obtained with mixing times of 100, 200, 300, and 500 ms at 5 °C. The ROESY spectrum was obtained with a mixing time of 500 ms at 5 and 25 °C. Five

hundred twelve increments of 2K data points were recorded with 32–96 transients for the TOCSY, NOESY, and ROESY experiments. The solvent resonance was suppressed by selective irradiation during a relaxation delay of 2.0 s. The  $^3J(\text{H-C}_\alpha\text{-C}_\beta\text{-H})$  measurement was carried out on an E.COSY spectrum recorded in  $\text{D}_2\text{O}$ . The chemical shifts were referenced with respect to  $\text{H}_2\text{O}$ , which in turn was calibrated using an internal standard, 2,2-dimethyl-2-silapentane-5-sulfonate, in a different sample. The chemical shift values of 4.95 and 4.75 ppm for the water signal were used at temperatures of 5 and 25 °C, respectively.

Interproton distance constraints were obtained from the NOESY spectra. Spin-diffusion effects were inspected by following the buildup of NOESY cross-peaks when mixing times were increased from 100 to 500 ms. The distance constraints were classified into four categories corresponding to 1.8–2.7, 1.8–3.5, 1.8–5.0, and 1.8–6.0 Å. Pseudoatoms were used for the prochiral methylene protons that had not been assigned in a stereospecific way, the methyl groups of the Ala and Leu residues and the  $\text{C}_\alpha$  proton of the Gly residues.<sup>50</sup> Correction factors for the use of pseudoatoms were added to the distance constraints. In addition, 0.5 Å was added to the distance constraints involving methyl protons. All calculations were performed on a Silicon Graphics Octane workstation with the X-PLOR program.<sup>51</sup> The dynamical simulated annealing protocols were used to calculate the 3D structures.

**Acknowledgment.** This study was partially supported by the Japan Science and Technology Agency.

## References

- Angel, P.; Karin, M. The Role of Jun, Fos and the AP-1 Complex in Cell-Proliferation and Transformation. *Biochim. Biophys. Acta* **1991**, *1072*, 129–157.
- Foletta, V. C.; Segal, D. H.; Cohen, D. R. Transcriptional Regulation in the Immune System: All Roads Lead to AP-1. *J. Leukocyte Biol.* **1998**, *63*, 139–152.
- Angel, P.; Baumann, I.; Stein, B.; Delius, H.; Rahmsdorf, H. J.; Herrlich, P. 12-*O*-Tetradecanoyl-Phorbol-13-Acetate Induction of the Human Collagenase Gene Is Mediated by an Inducible Enhancer Element Located in the 5'-Flanking Region. *Mol. Cell. Biol.* **1987**, *7*, 2256–2266.
- Suto, M. J.; Ransone, L. J. Novel Approaches for the Treatment of Inflammatory Diseases: Inhibitors of NF- $\kappa$ B and AP-1. *Curr. Pharm. Des.* **1997**, *3*, 515–528.
- Shiozawa, S.; Shimizu, K.; Tanaka, K.; Hino, K. Studies on the Contribution of c-fos/AP-1 to Arthritic Joint Destruction. *J. Clin. Invest.* **1997**, *99*, 1210–1216.
- Kouzarides, T.; Ziff, E. The Role of the Leucine Zipper in the Fos-Jun Interaction. *Nature* **1988**, *336*, 646–651.
- Glover, J. N. M.; Harrison, S. C. Crystal Structure of the Heterodimeric bZIP Transcription Factor c-Fos-c-Jun Bound to DNA. *Nature* **1995**, *373*, 257–261.
- Patel, L.; Abate, C.; Curran, T. Altered Protein Conformation on DNA Binding by Fos and Jun. *Nature* **1990**, *347*, 572–575.
- Saudek, V.; Pastore, A.; Morelli, M. A. C.; Frank, R.; Gausepohl, H.; Gibson, T.; Weih, F.; Roesch, P. Solution Structure of the DNA-Binding Domain of the Yeast Transcriptional Activator Protein GCN4. *Protein Eng.* **1990**, *4*, 3–10.
- Gohlke, H.; Klebe, G. Approaches to the Description and Prediction of the Binding Affinity of Small-Molecule Ligands to Macromolecular Receptors. *Angew. Chem., Int. Ed.* **2002**, *41*, 2644–2676.
- Davis, A. M.; Teague, S. J.; Kleywegt, G. J. Application and Limitations of X-ray Crystallographic Data in Structure-Based Ligand and Drug Design. *Angew. Chem., Int. Ed.* **2003**, *42*, 2718–2736.
- Lee, S.; Park, S.; Jun, G.; Hahm, E.-R.; Lee, D.-K.; Yang, C.-H. Quantitative Assay for the Binding of Jun-Fos Dimer and Activator Protein-1 Site. *J. Biochem. Mol. Biol.* **1999**, *32*, 594–598.
- Hahm, E.-R.; Cheon, G.; Lee, J.; Kim, B.; Park, C.; Yang, C.-H. New and Known Symmetrical Curcumin Derivatives Inhibit the Formation of Fos-Jun-DNA Complex. *Cancer Lett.* **2002**, *184*, 89–96.
- Park, S.; Lee, D.-K.; Yang, C.-H. Inhibition of Fos-Jun-DNA Complex Formation by Dihydroguaiaretic Acid and in Vitro Cytotoxic Effects on Cancer Cells. *Cancer Lett.* **1998**, *127*, 23–28.
- Park, S.; Lee, D. K.; Whang, Y. H.; Yang, C. H. Momordin I, a Compound of Ampelopsis Radix, Inhibits AP-1 Activation Induced by Phorbol Ester. *Cancer Lett.* **2000**, *152*, 1–8.
- Goto, M.; Masegi, M.; Yamauchi, T.; Chiba, K.; Kuboi, Y.; Harada, K.; Naruse, N. K1115 A, a New Anthraquinone Derivative that Inhibits the Binding of Activator Protein-1 (AP-1) to its Recognition Sites. *J. Antibiot.* **1998**, *51*, 539–544.
- Ghose, A. K.; Wendoloski, J. J. Pharmacophore Modelling: Methods, Experimental Verification and Applications. *Perspect. Drug Discovery Des.* **1998**, 253–271.
- Hruby, V. J. Conformational and Topographical Considerations in the Design of Biologically Active Peptides. *Biopolymers* **1993**, *33*, 1073–1082.
- Li, P.; Roller, P. P. Cyclization Strategies in Peptide Derived Drug Design. *Curr. Top. Med. Chem.* **2002**, *2*, 325–341.
- SYBYL 6.4; Tripos, Inc.: St. Louis, MO, 1997.
- Nakabeppu, Y.; Nathans, D. The Basic Region of Fos Mediates Specific DNA Binding. *EMBO J.* **1989**, *8*, 3833–3841.
- Turner, R.; Tjian, R. Leucine Repeats and an Adjacent DNA Binding Domain Mediate the Formation of Functional cFos-cJun Heterodimers. *Science* **1989**, *243*, 1689–1694.
- Gentz, R.; Rauscher, F. J., III; Abate, C.; Curran, T. Parallel Association of Fos and Jun Leucine Zippers Juxtaposes DNA Binding Domains. *Science* **1989**, *243*, 1695–1699.
- Neuberg, M.; Schuermann, M.; Hunter, J. B.; Müller, R. Two Functionally Different Regions in Fos are Required for the Sequence-Specific DNA Interaction of the Fos/Jun Protein Complex. *Nature* **1989**, *338*, 589–590.
- Risse, G.; Jooss, K.; Neuberg, M.; Brüller, H.-J.; Müller, R. Asymmetrical Recognition of the Palindromic AP1 Binding Site (TRE) by Fos Protein Complexes. *EMBO J.* **1989**, *8*, 3825–3832.
- Ransone, L. J.; Visvader, J.; Wamsley, P.; Verma, I. M. Trans-Dominant Negative Mutants of Fos and Jun. *Proc. Natl. Acad. Sci. U.S.A.* **1990**, *87*, 3806–3810.
- Clark, M.; Cramer, R. D., III; Van Opdenbosch, N. Validation of the General Purpose Tripos 5.2 Force Field. *J. Comput. Chem.* **1989**, *10*, 982–1012.
- Gasteiger, J.; Marsili, M. Iterative Partial Equalization of Orbital Electronegativity—A Rapid Access to Atomic Charges. *Tetrahedron* **1980**, *36*, 3219–3228.
- Purcell, W. P.; Singer, J. A. A Brief Review and Table of Semiempirical Parameters Used in the Hückel Molecular Orbital Method. *J. Chem. Eng. Data* **1967**, *12*, 235–246.
- Pearlman, D. A.; Case, D. A.; Caldwell, J. W.; Ross, W. S.; Cheatham, T. E., III; Ferguson, D. M.; Seibel, G. L.; Singh, U. C.; Weiner, P.; Kollman, P. A. *AMBER 4.1*; University of California: San Francisco, CA, 1995.
- Jorgensen, W. L.; Chandrasekhar, J.; Madura, J. D.; Impey, R. W.; Klein, M. L. Comparison of Simple Potential Functions for Simulating Liquid Water. *J. Chem. Phys.* **1983**, *79*, 926–935.
- Ryckaert, J.-P.; Ciccotti, G.; Berendsen, H. J. C. Numerical Integration of the Cartesian Equations of Motion of a System with Constraints: Molecular Dynamics of *n*-Alkanes. *J. Comput. Phys.* **1977**, *23*, 327–341.
- Peeters, T. L.; Macielag, M. J.; Depoortere, I.; Konteatis, Z. D.; Florance, J. R.; Lessor, R. A.; Galdes, A. D-Amino Acid and Alanine Scans of the Bioactive Portion of Porcine Motilin. *Peptides* **1992**, *13*, 1103–1107.
- Tam, J. P.; Liu, W.; Zhang, J.-W.; Galantino, M.; Bertolero, F.; Cristiani, C.; Vaghi, F.; De Castiglione, R. Alanine Scan of Endothelin: Importance of Aromatic Residues. *Peptides* **1994**, *15*, 703–708.
- Sahm, U. G.; Olivier, G. W. J.; Branch, S. K.; Moss, S. H.; Pouton, C. W. Synthesis and Biological Evaluation of  $\alpha$ -MSH Analogues Substituted with Alanine. *Peptides* **1994**, *15*, 1297–1302.
- Leprince, J.; Gandolfo, P.; Thoumas, J.-L.; Patte, C.; Fauchère, J.-L.; Vaudry, H.; Tonon, M.-C. Structure–Activity Relationships of a Series of Analogues of the Octadecaneuropeptide ODN on Calcium Mobilization in Rat Astrocytes. *J. Med. Chem.* **1998**, *41*, 4433–4438.
- Wüthrich, K. *NMR of Proteins and Nucleic Acids*; John Wiley & Sons: New York, 1986.
- Rance, M.; Sørensen, O. W.; Bodenhausen, G.; Wagner, G.; Ernst, R. R.; Wüthrich, K. Improved Spectral Resolution in COSY  $^1\text{H}$  NMR Spectra of Proteins via Double Quantum Filtering. *Biochem. Biophys. Res. Commun.* **1983**, *117*, 479–485.
- Bax, A.; Davis, D. G. MLEV-17-Based Two-Dimensional Homonuclear Magnetization Transfer Spectroscopy. *J. Magn. Reson.* **1985**, *65*, 355–360.
- Macura, S.; Huang, Y.; Suter, D.; Ernst, R. R. Two-Dimensional Chemical Exchange and Cross-Relaxation Spectroscopy of Coupled Nuclear Spins. *J. Magn. Reson.* **1981**, *43*, 259–281.
- IUPAC-IUB Joint Commission on Biochemical Nomenclature (JCBN) Nomenclature and Symbolism for Amino Acids and Peptides. *J. Biol. Chem.* **1985**, *260*, 14–42.
- Merrifield, R. B. Solid Phase Peptide Synthesis. I. The Synthesis of a Tetrapeptide. *J. Am. Chem. Soc.* **1963**, *85*, 2149–2154.

- (43) Carpino, L. A.; Han, G. Y. The 9-Fluorenylmethoxycarbonyl Amino-Protecting Group. *J. Org. Chem.* **1972**, *37*, 3404–3409.
- (44) Rink, H. Solid-Phase Synthesis of Protected Peptide Fragments Using a Trialkoxy-Diphenyl-Methylester Resin. *Tetrahedron Lett.* **1987**, *28*, 3787–3790.
- (45) Otaka, A.; Koide, T.; Shide, A.; Fujii, N. Application of Dimethylsulphoxide (DMSO)/Trifluoroacetic Acid (TFA) Oxidation to the Synthesis of Cystine-Containing Peptide. *Tetrahedron Lett.* **1991**, *32*, 1223–1226.
- (46) Dignam, J. D.; Lebovitz, R. M.; Roeder, R. G. Accurate Transcription Initiation by RNA Polymerase II in a Soluble Extract from Isolated Mammalian Nuclei. *Nucleic Acids Res.* **1983**, *11*, 1475–1489.
- (47) Bax, A.; Davis, D. G. Practical Aspects of Two-Dimensional Transverse NOE Spectroscopy. *J. Magn. Reson.* **1985**, *63*, 207–213.
- (48) Griesinger, C.; Sørensen, O. W.; Ernst, R. R. Practical Aspects of the E.COSY Technique. Measurement of Scalar Spin–Spin Coupling Constants in Peptides. *J. Magn. Reson.* **1987**, *75*, 474–492.
- (49) States, D. J.; Haberkorn, R. A.; Ruben, D. J. A Two-Dimensional Nuclear Overhauser Experiment with Pure Absorption Phase in Four Quadrants. *J. Magn. Reson.* **1982**, *48*, 286–292.
- (50) Wüthrich, K.; Billeter, M.; Braun, W. Pseudo-Structures for the 20 Common Amino Acids for Use in Studies of Protein Conformations by Measurements of Intramolecular Proton–Proton Distance Constraints with Nuclear Magnetic Resonance. *J. Mol. Biol.* **1983**, *169*, 949–961.
- (51) Brünger, A. T. *X-PLOR version 3.1*; Yale University: New Haven, CT, 1993.

JM049890+